Evaluation of Gait Transitional phases using Neuromechanical outputs and somatosensory inputs in an Overground walk

Imran Mahmood [a, 1], Uriel Martinez-Hernandez [b], Abbas A. Dehghani-Sanij [a]

[a] Institute of Design, Robotics, and Optimisation, School of Mechanical Engineering
University of Leeds, Leeds, United Kingdom

[b] Department of Electronic and Electrical Engineering,
University of Bath, Bath, United Kingdom

Submitting for Original Article

[1] Corresponding Author
Imran Mahmood
School of Mechanical Engineering
The University of Leeds,
Leeds, LS2 9JT, United Kingdom
Email: mnim@leeds.ac.uk
Phone +44(0)7589658714

Abstract

In a bipedal walk, the human body experiences continuous changes in stability especially during weight loading and unloading transitions which are reported crucial to avoid fall. Prior stability assessment methods are unclear to quantify stabilities during these gait transitions due to methodological and/or measurement limitations. This study introduces Nyquist and Bode methods to quantify stability gait transitional stabilities using the neuromechanical output (CoP) and somatosensory input (GRF) responses. These methods are implemented for five different walking conditions grouped into walking speed and imitated rotational impairments. The trials were recorded with eleven healthy subjects using motion cameras and force platforms. The time rate of change in O/Is illustrated impulsive responses and modelled in the frequency domain. Nyquist and Bode stability methods are applied to quantify stability margins. Stability margins from outputs illustrated loading phases as stable and unloading phases as unstable in all walking conditions. There was a strong intralimb compensatory interaction ($p<0.001$, Spearman correlation) found between opposite limbs. Overall, both walking groups illustrated a decrease ($p<0.05$, Wilcoxon signed-rank test) in stability margins compared with normal/preferred speed walk. Further, stabilities quantified from outputs were found greater in magnitudes than the instability quantified from inputs illustrating the neuromotor balance control ability. These stability outcomes were also compared by applying extrapolated-CoM method. These methods of investigating gait dynamic stability are considered as having important implications for the assessment of ankle-foot impairments, rehabilitation effectiveness, and wearable orthoses.

Key words: Gait, transitional phases, dynamic stability, Nyquist and Bode, neuromotor

Research Highlights

- Gait dynamic stability evaluated during loading and unloading transitions
- Neuromotor output and inputs measured from CoP and CoM-acceleration signals
- Nyquist and Bode methods introduced to quantify gait transitional stabilities
- Eversion and inversion foot impairments illustrated a significant decrease in stability
- Overground walking speeds partially impacted on gait transitional stabilities

1. Introduction

Gait dynamic stability is important for independence while performing daily living activities. Various stability assessment techniques are reported earlier mainly categorised into clinical and laboratory-based methods (Neptune & Vistamehr, 2018). Clinically, walking stabilities are assessed applying Berge balance, Time up and go tests in which questionnaires are used or stopwatch measurements are made from patients. Laboratory-based methods involve sophisticated equipment and are reported with precise quantification of gait dynamic stabilities. Laboratory methods are further categorised into discrete point or continuous time series stability evaluations of a gait cycle using related measurement signals. Laboratory methods are not yet being applied in clinical environments due to diversified outcomes and multiple biomechanical signals being used. Further, the stability evaluation criteria in these methods are based on a comparison between testing and control subjects to define a gait being stable or unstable.

Considering methodological choices, firstly, the discrete events stability evaluations include lower limb joints peak angles and moments (Soares, de Castro, Mendes, & Machado, 2014), spatiotemporal parameters (step width, step length), or extrapolated center-of-mass (XCoM) difference from base-of-support (BoS) (Hof, 2008; Sivakumaran, Schinkel-Ivy, Masani, & Mansfield, 2018). In the second category, stability evaluations involve continuous time series bulk data of measurement waveforms, these include, Lyapunov exponent, Floquet multiplier, (Ihlen et al., 2012; Kang & Dingwell, 2009) and intraclass correlation methods (Rabuffetti et al., 2011). These methods were used to quantify gait stabilities as a unit-less factor which was assumed consistent over the entire stride. Both these discrete and continuous time series methods are being indistinct to evaluate gait transitional phases i.e. loading and unloading phases which are reported critical considering gait dynamic stabilities (Bizovska et al., 2014; Svoboda et al., 2017). The loading and unloading phases include ~30% of stance from heel contact and towards toe-off events respectively, also known as double limb support time in a gait cycle. During these transitions, body weight is transferred from one limb to others (Bizovska et al., 2014), neuromotor programs is modulated (Rabuffetti et al., 2011), and muscles activate to maximum level to provide acceleration to trailing limb and decelerate to the leading limb (La Scaleia, Ivanenko, Zelik, & Lacquaniti, 2014). Despite these vital biological transformations taking place during these phases, the gait dynamic stabilities have been remained unquantified during these gait phases.

Considering measurement signals, prior methods used multiple variables to evaluate gait stabilities. For example, most widely used extrapolated-CoM (XCoM) method attempt to quantify BoS from different foot positions, these include, foot centre of pressure (CoP) trajectory, toe marker, or heel marker positions. This method quantifies margins of stability (MoS) as XCoM maximum sways from BoS at HC and TO events and assumes double limb support time zero (Hof, 2008). Another most reliable method ‘Lyapunov exponent’ is reported to use multiple variables e.g. markers positions data from either trunk, pelvis, lower limb segments, joints, EMGs or their higher order derivatives to evaluate dynamic stability. A few studies are also reported to have criteria of at least five variables needed in the Lyapunov exponent method to be precise (Kang & Dingwell, 2009). In comparison, the neuromotor balance control theory states that lower limb muscles activate in response to CoM positions or acceleration (Allen & Ting, 2016; Graham, Carty, Lloyd, & Barrett, 2017) and CoP gives measure of resultant neuromotor balance control (Lugade & Kaufman, 2014), however, CoP is

independent to that of CoM (Winter, 2009). Despite the use of body's CoP and CoM being widely reported in relation to stability evaluation, their application for gait transitional phases stability evaluation has been remained uninvestigated due to methodological limitations.

More recent studies have introduced Nyquist and Bode (N&B) methods to quantify gait dynamics stabilities related to knee deficiencies (Ardestani, ZhenXian, Noori, Moazen, & Jin, 2019; Morgan, Zheng, Bush, & Noehren, 2016) and postural perturbations (Hur, Duiser, Salapaka, & Hsiao-Wecksler, 2010). These are control engineering stability analysis techniques with the capability of evaluating transient and steady-state stabilities. Earlier, these methods were widely used for design and control in medical robots, however, their application in gait stability evaluations is relatively new. In this study, we have applied these methods using resultant ground reaction forces (GRF) biomechanical signals such that the tail of GRF vector presents CoP (output) and head of GRF vector presents CoM-acceleration (input) responses by the neuromotor (Appendix Fig. A1). These methods are implemented here specifically for stability evaluations during gait transitional phases.

2. Methods

2.1. Participants

A total of eleven healthy subjects participated in this study (age 30±1yr, weight 74±3kg, and height 1.72±2.5m) after confirming no prior anatomical or neuromuscular impairments. Each subject signed an informed consent form which was approved by the institutional ethical review board at the University of Leeds.

2.2. Experimental Protocol

Two different walking conditions i.e. preferred walking speeds and rotational impairments are simulated in this study to evaluate gait transitional stabilities. Following prior studies (Rabiei, Eslami, & Movaghar, 2016; Soares et al., 2014), the rotational foot impairments were imitated using self-designed wedge-shaped foot insoles (Fig. A3). The insoles were designed in pairs using Styrofoam sheet (high density, thickness 1inch, compressive strength 690kPa) and wedged to ±10° using a hot wire cutter. The Styrofoam material preserves the loading impacts compared to commercially available soft insoles and helps in imitating eversion and inversion foot deficiencies. In this study, these foot conditions were imitated to a moderate range i.e. -10° laterally inclined insole for inverted/supinated foot and +10° medially inclined insole for the everted/pronated foot. Each insole was further cut into two parts i.e. hindfoot and forefoot to allow forefoot flexible motion during the push-off phase. Both parts were joined together using gaffer tape. These insoles were made portable to perform dynamic activities and worn by each participant using Velcro straps.

2.3. Data Collection

The trials were conducted in motion capture lab using 12 infrared cameras (Oqus cameras, 400 Hz), two force platforms (AMTI BP400600-2000, 1 kHz), and 26 reflective markers were attached to each subject at lower limbs as illustrated in Fig. A1. The placement of the markers was made following Visual-3D help document (C-Motion_Markers, 2019) as illustrated in Fig. A2. There are two distinct force plates mounted on the lab floor in the pathway. The subjects were instructed to adjust their steps to ensure each foot was positioned at a separate force plate. After getting familiar, the experiments were recorded using Qualisys software. Each force plate

measures three-dimensional (3D) ground reaction forces (GRFs) and two-dimensional (2D) centre of pressure (CoP) position trajectories. The recorded data from each foot was used for further analysis. Each subject performed five trials for each of the five walking conditions. These five walking conditions were further grouped into walking speed (slow, normal and fast) and rotational foot impairments (everted and inverted foot). A self-selected normal speed walk was considered as a reference in both groups. The sequence in which trials were recorded included slow, normal, and fast speed trials at first and thereafter imitated inverted and everted foot walking conditions were performed at a self-selected preferred walking speed. While simulating rotational foot impairments, each subject was asked to get familiar by walking with wedged insoles in both feet, and after feeling comfortable, the trials were recorded. The trials were recorded on an 8m walking track. During each trial, the data from the limb movements were recorded in terms of 3D marker coordinates, 3D GRFs, and 2D CoP-position. Markers coordinates were used to compute ankle-foot angles and margin-of-stability (MoS). The GRFs and CoP position data were used to evaluate stability margins in anterior-posterior and medial-lateral directions.

2.4. Data Processing

The rotational ankle-foot angles for simulated walking conditions were computed in the Visual-3D motion analysis software (Fig. A4) following the procedure defined in the software's help document (C-Motion_Angles, 2019). Firstly, lower-limb markers position data was exported to Visual-3D software as C3D files. Each C3D file includes 26 markers (x, y, z) coordinates those were attached to foot, ankle and shank segments. Secondly, this data was used to construct the body's anatomical model, and finally, a built-in command used to compute rotation of foot w.r.t shank reference. The rotation of foot w.r.t shank measures ankle joint angles along (x, y, z) directions. The rotational angles present the rotation of ankle-foot along the anterior-posterior axis of the ankle-foot joint. An outward ankle-foot rotation is called inversion and an inward rotation is called eversion. The outcomes from everted/inverted foot simulations abnormalities (using ±10° wedged insoles) were further confirmed by evaluating ankle-foot rotational angles experimentally in Visual-3D. Fig. 4 illustrates the trajectories (mean±Std.) for the normal, everted and inverted foot conditions. A maximum difference of everted and inverted foot trajectories was computed w.r.t to the normal foot trajectory. These differences in rotational angles were found as 6.66°(±2.67) for the everted foot and 6.77°(±2.49) for an inverted foot condition. These experimentally obtained rotational angles are in approximation to the wedged angles of wearable insoles. These ranges imitate moderate range rotational impairments and are consistent with a previous study (Rabiei et al., 2016). The ground reaction force (GRF) and CoP raw data were exported directly to MATLAB-2017a. The anterior-posterior and medial-lateral components of both of these two signals were processed further. For each of the individual subjects, the GRF (Newton) data recorded during each trial was normalised by the respective subject's body mass (kg) to obtain CoM-acceleration (i.e. GRF/mass). For each of the measured signals, both the amplitude and respective time axes information was used for further processing. The time rate of change of CoP and CoM-acceleration were computed. In each trial, both amplitude and time axes were recorded for the whole stance phase which was further analysed by diving stance into subphases (i.e. loading and unloading). These sub-phases also present initial and ending double limb support phases of a gait cycle (Bizovska et al., 2014). The input data set for each of the measured signals consist of (100 samples × 55 trials). Equations (1-3) were applied to the rows

(i.e. samples in each column) such that two consecutive samples were used to compute mean CoP-velocity and RMS CoM-oscillations for respective input signals. For each trial, at first, equation (1) was applied to compute actual CoP-velocity and thereafter equation (2) was applied to compute mean values of the actual CoP-velocities following (Bizovska et al., 2014; ImageJ-macros, 2019; Mei et al., 2013). The averaging of actual CoP-velocity applying Eq. 2 helps to smoothen the noise as also illustrated in Fig. 1(a). Similarly, equations (1) and (3) were used to compute the rate of change in CoM-acceleration and RMS CoM-oscillations following (Cattaneo et al., 2014; Rabuffetti et al., 2011).

$$V_{COP\_actual} = \frac{d_{xi}}{d_{ti}} = \frac{|y_{i+1} - y_i|}{|t_{i+1} - t_i|} \quad (1)$$

$$V_{COP\_average} = \frac{d_{xi} + d_{x\_sum}}{d_{ti} + d_{t\_sum}} \quad (2)$$

Where $'d_{xi}'$ and $'d_{ti}'$ are the differences between two consecutive samples measuring CoP positions i.e. y_i, y_{i+1} and time samples i.e. t_i, t_{i+1}. Similarly, $'d_{x\_sum}'$ and $'d_{t\_sum}'$ present the sum of previous differences and current samples difference.

$$\dot{a_{CoM}} = \sqrt{(\dot{a_1}^2 + \dot{a_2}^2)/2} \quad (3)$$

Where $'\dot{a_{CoM}}'$ presents RMS value of CoM-oscillation, $'\dot{a_1}'$ and $'\dot{a_2}'$ are the rate-of-change of CoM-acceleration and present two consecutive samples of a waveform.

During the loading phases, both signals (mean CoP-velocity and RMS CoM-oscillations) showed the instant rise and thereafter exponential decay in magnitudes. Oppositely during respective unloading phases, an exponential rise and thereafter an instant decay was observed in the measurement signals as illustrated in Fig.1. Following engineering control theory, a linear dynamic system that illustrates the aforementioned signal characteristics is considered as an output response to the unit impulse input. That unit input assumption helps in identifying the best-fit model by applying reverse engineering i.e. model identification approach as reported previously (Anderson et al., 2009; Morgan et al., 2016). These impulsive responses were windowed such that initial 30% of stance from HC presented as loading phase and last 30% towards toe-off presented as unloading phase (Bizovska et al., 2014). The mean CoP-velocity impulses were filtered applying first-order Butterworth at 30Hz following (van der Linden, van der Linden, Hendricks, van Engelen, & Geurts, 2010) and RMS CoM-oscillations were filtered using second-order Butterworth at 10Hz (Sivakumaran et al., 2018).

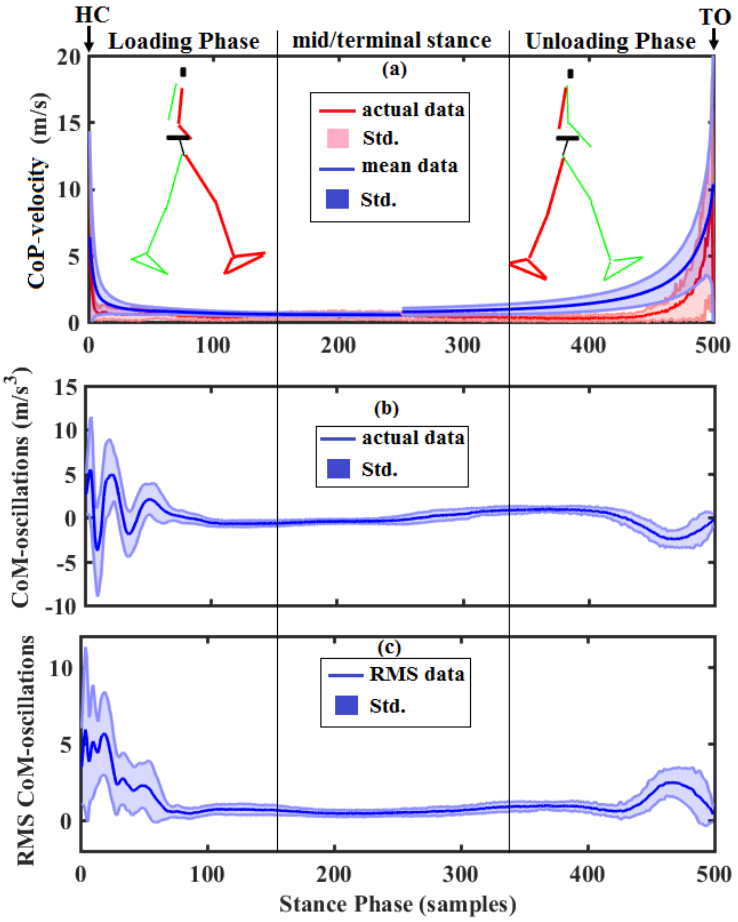

Fig. 1. Impulsive waveforms during gait transitions. The time rate of change in CoP and CoM-acceleration illustrated during loading and unloading phases for normal speed trials in the anterior-posterior direction. For each of the actual, mean, and RMS plots of respective signals, each data set present mean±Std. for 55 trials (i.e. 11 subjects × 5 trials). (a) CoP-velocity actual and mean data, (b) CoM-oscillations actual data, (c) Root-mean-square (RMS) values of CoM-oscillations.

Following neuromotor balance control, in this study, the CoP and CoM-oscillations are modelled as output and input responses respectively as shown in Fig. 2. It is widely reported earlier that any change in the body's CoM-acceleration acts as a feedback to reweight neuromotor control to activate lower limb muscles (Allen & Ting, 2016; Blum, Lamotte D'Incamps, Zytnicki, & Ting, 2017; La Scaleia et al., 2014). Similarly, the CoP is reported as a measure of neuromuscular control towards posture and gait (Lugade & Kaufman, 2014; Portela, Rodrigues, & de Sá Ferreira, 2014; Winter, 2009), however, the CoP trajectory is independent to the CoM. Following these well-known facts, we have modelled and analysed both signals independently. Also, prior studies analysed CoP (Bizovska et al., 2014; DiDomenico, McGorry, & Banks, 2013; Lugade & Kaufman, 2014) and CoM-acceleration (Cattaneo et al., 2014; Lencioni et al., 2014; Rabuffetti et al., 2011) signals independently while evaluating gait dynamic stability. A detailed neuromotor balance control loop is constructed in Fig. 2 with all constituent components. Considering neuromotor feedbacks, CoM-oscillations are reported as major somatosensory feedback that counts almost 70% along with vision and hearing those contribute 30% in overall (Bekkers et al., 2014). Summarising, CoP reflects changes in neuromotor independently in Fig. 2 and CoM-oscillations acts as a biomechanical

trigger to whom neuromotor respond. One requirement of applying N&B analyses techniques is the linear time-invariant models of the measuring system. The resultant waveforms (i.e. mean CoP-velocity and RMS CoM-oscillations) illustrated artefacts due to repeated trials performed with multiple subjects which included differences in anthropological data, markers adjustments and foot insoles placements. These artefacts induce non-linearity in the data, hence, cleaned by applying principal component analysis (PCA) following earlier studies (Anderson et al., 2009; Sklavos, Porrill, Kaneko, & Dean, 2005; Tan & Hammond, 2007). The PCA transform the output data as a linear combination of involved variables, implemented here for individual walking conditions and transitional phases following (Maslivec et al., 2018).

The time-series waveforms for both loading and unloading phases were cleaned from artefacts by applying PCA. The methodological choice of PCA is adapted from earlier studies (Anderson et al., 2009; Maslivec et al., 2018; Robbins, Astephen Wilson, Rutherford, & Hubley-Kozey, 2013). Also, the Inspect 3D software (Inspect3D, 2018) was used for repeated measure data artefacts removal, however, we implemented PCA using MATLAB. The input variables are mean CoP-velocity and RMS CoM-oscillations. Each of the repeatedly measured variables consists of time-series waveforms data (input matrix:100×55), where 100 presents samples per trial and 55 presents the total number of trials (11 subjects×5 trials). PCA converts measured waveforms into various time dimensions also known as orthogonal signals (Cohen, 2014). The variance in these repeatedly measured input waveforms is described along each time dimension also known as principal components (orthogonalized signals). General criteria reported earlier is that the PCs should be used which explained at least 80% of the variability (Robbins et al., 2013).

In this study, principal components (PCs) that explain maximum variance (>90%) are used for reconstruction. For each variable, the output waveforms were reconstructed using $X=ZU^t$ (Z: score matrix, U: coefficient matrix, X: output matrix). The PCA performed here also helps to approximate the linear behaviour of time-series data that follows prior studies with similar changing period signal characteristics (Anderson et al., 2009; Downes et al., 2012; Sklavos et al., 2005). A low dimensionality in our data indicates a low-order linear model for the underlying system and any non-linearities are likely to be small. Hence, the least-square linear regression models are identified as best-fit to the measured waveforms. The mean of each subject's reconstructed waveforms (trials) was used in subsequent analysis.

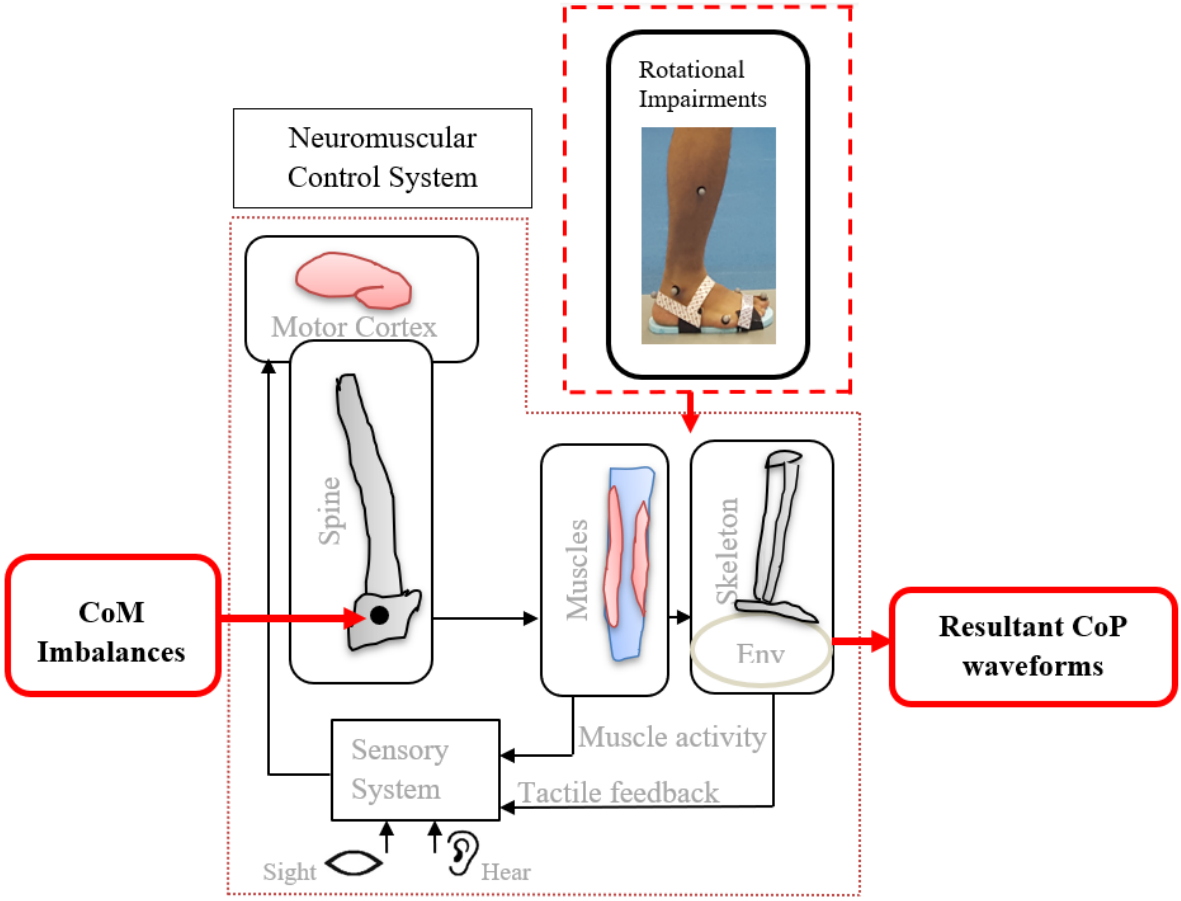

Fig. 2. Neuromotor balance control illustrated using resultant biomechanical signals. The CoM imbalances quantified as CoM-oscillations (rate-of-change in CoM-acceleration) acts as somatosensory input that acts as a feedback to reweight muscles activity at the onset of the perturbations. The centre-of-pressure (CoP) measures resultant neuromuscular response towards posture and gait, independent to the centre-of-mass (CoM).

2.5. Frequency domain Transfer Functions (TFs)

The loading and unloading phases reconstructed waveforms were modelled using least square linear regression technique. A sum of exponent models was found the best fit (R^2: 99±0.5%) for CoP-velocity and a sum of sinusoidal functions was found the best fit (R^2: 99±0.5%) for CoM-oscillations. These time-domain models were converted to frequency domain applying Laplace transformation in MATLAB-2017a following (Morgan et al., 2016) and resultant models are named as transfer functions (TF). A transfer function is the ratio of Laplace of output to input polynomials. The roots of numerator polynomial present zeros of a TF and roots of denominator polynomial present poles of a TF. If the poles lie on the left half of the s-plane the system is defined as stable, otherwise unstable.

2.6. Nyquist and Bode Stability Criteria

Nyquist and Bode methods are implemented by assuming linear time-invariant models as illustrated by low dimensionality (PCA) in the input waveforms for both mean CoP-velocity and RMS CoM-oscillations. Both of these two signals quantify resultant effects of whole limb motions, hence, non-linearities in CoM-oscillations caused by mass-inertia changes around the individual joints (ankle, knee and hip) are likely to be small. These open-loop TFs modelled

from CoP-velocity and CoM-oscillations were excited by unit impulse input perturbations (Morgan et al., 2016) and stability margins were quantified following Nyquist and Bode stability criteria (Bavafa-Toosi, 2017). The Nyquist plot presents a TF/model in a polar plot in which the point (-1, 0j) is used to define critical stability. The difference of a system's gain and phase plots from this critical point is used to quantify stability as gain margin (GM) and phase margin (PM) (Fig. A5). The gain margin (decibel/dB) presents the magnitude of a system's gain at a frequency where the corresponding phase plot cuts $\pm 180° \pm 2k\pi$ axes (Bavafa-Toosi, 2017). Similarly, the phase margin (degrees) presents the magnitude of a phase at a frequency where the corresponding gain plot cuts the 0dB axis. In control theory, a GM measures robustness of a system and a PM measures the stability of a dynamic system. These margins present the difference from an unstable region if a system is stable, conversely these present the distance from a stable region if a system is unstable. A system might have multiple gain and phase margins, however, the smallest of them is considered critical as it is closest to instability region if presented for a stable system, and vice-versa (Bavafa-Toosi, 2017).

2.7 Extrapolated-CoM difference from BoS

For comparing between gait events and phases stabilities, the discrete events based MoS(s) were also evaluated by computing extrapolated-CoM (XCoM) and BoS following the methods used by (Lugade, Lin, & Chou, 2011; Sivakumaran et al., 2018). The XCoM difference from BoS boundary (CoP position) was computed at heel contact (HC) and toe-off (TO) events in both anterior-posterior and medial-lateral directions. The MoS(s) at HC presents the starting point of a loading phase and at TO event presents ending point of an unloading phase. A decrease in MoS(s) gives an indication of poor balance control, however, in some cases, an increase in XCoM movement w.r.t BoS at toe-off also indicates poor balance control (Lugade et al., 2011). In this study, a decrease in MoS(s) at toe-off event is considered as an indication of poor balance control compared with control subjects trials at normal speed.

2.8 Statistical Comparison

After analysing the modelled TFs, the stability outcomes i.e. GM, PM, and MoS are tested for the normality applying Shapiro-Wilk test. Observing non-normality in the data ($p<0.05$), the Wilcoxon signed-rank test was applied in SPSS (version 23, Chicago, IL, USA) to compare stability outcomes between simulated walking conditions and a normal walk. A parameter was considered statistically significant if $p<0.05$. Also, both mean CoP-velocity and RMS CoM-oscillation waveforms illustrated non-normal distribution. Hence, the Spearman's correlations were evaluated between intralimb mean CoP-velocities (O/P), and between mean CoP-velocity (O/P) and RMS CoM-oscillations (I/P).

3. Results

The best fit models to CoP-velocity (O/P) waveforms illustrated stable responses in loading phases and unstable responses during unloading phases. Considering rotational impairments, the stability (PM) decreased ($p<0.05$) in both everted and inverted foot walks during loading phases (Fig. 3a) and instability (GM, PM) decreased ($p<0.05$) in an inverted foot alone during respective unloading phases (Fig. 4a, Table A1) in anterior-posterior (AP) direction. In medial-lateral (ML) direction, both rotational impairments showed a decrease ($p<0.05$) in stability (Fig. 3c), however, there was no significant difference found during unloading phases (Fig. 4c). Considering walking speed group, the stability (PM) decreased ($p<0.05$) at slow speed in

loading phase (Fig. 3e and 3g) and instability (GM, PM) decreased ($p<0.05$) at fast speed during unloading phases (Fig. 4e and 4g).

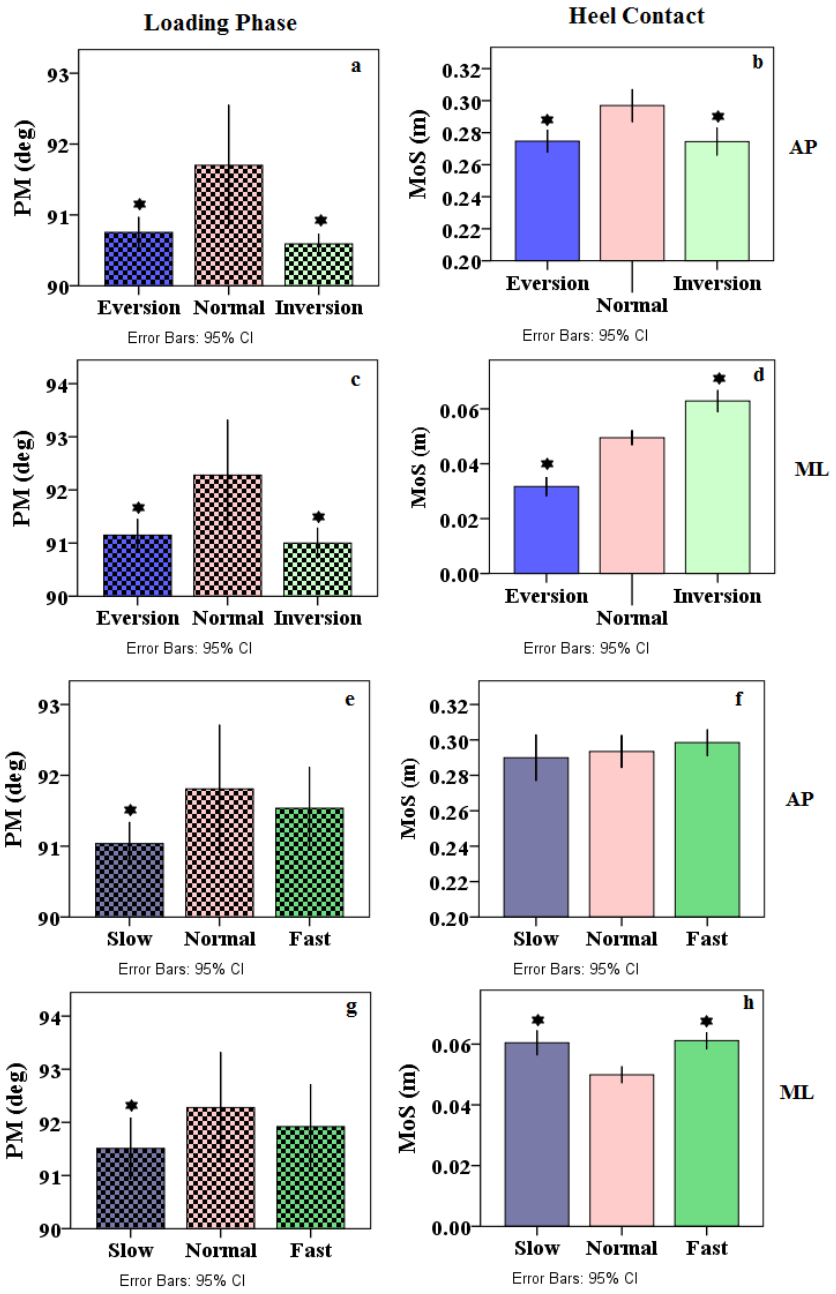

Fig. 3. Stability margins comparison during loading phases applying N&B methods (left) and extrapolated-CoM method (right). (a-d) rotational impairments in anterior-posterior (AP) and medial-lateral (ML) directions, (e-h) walking speed group in AP and ML directions, * shows significant ($p<0.05$) difference.

Considering rotational impairments, in AP direction, both eversion and inversion conditions showed a decrease ($p<0.05$) in MoS(s) at HC (Fig. 3b, Table A1) and TO (Fig. 4b, Table A1). In ML direction, an inverted foot walk illustrated an increase in MoS(s) at both HC (Fig. 3d) and TO (Fig. 4d) events. An everted foot showed a decrease in MoS only at HC (Fig. 3d). The MoS(s) quantified from the extrapolated-CoM method at HC showed no significant difference in walking speeds in AP direction (Fig. 3f), however, increased in ML direction (Fig. 3h). At

TO event, MoS decreased ($p<0.05$) at slow speed and increased at fast speed in AP direction compared to a normal walk (Fig. 4f). Both slow and fast speed walks illustrated increased MoS(s) in ML direction (Fig. 4h).

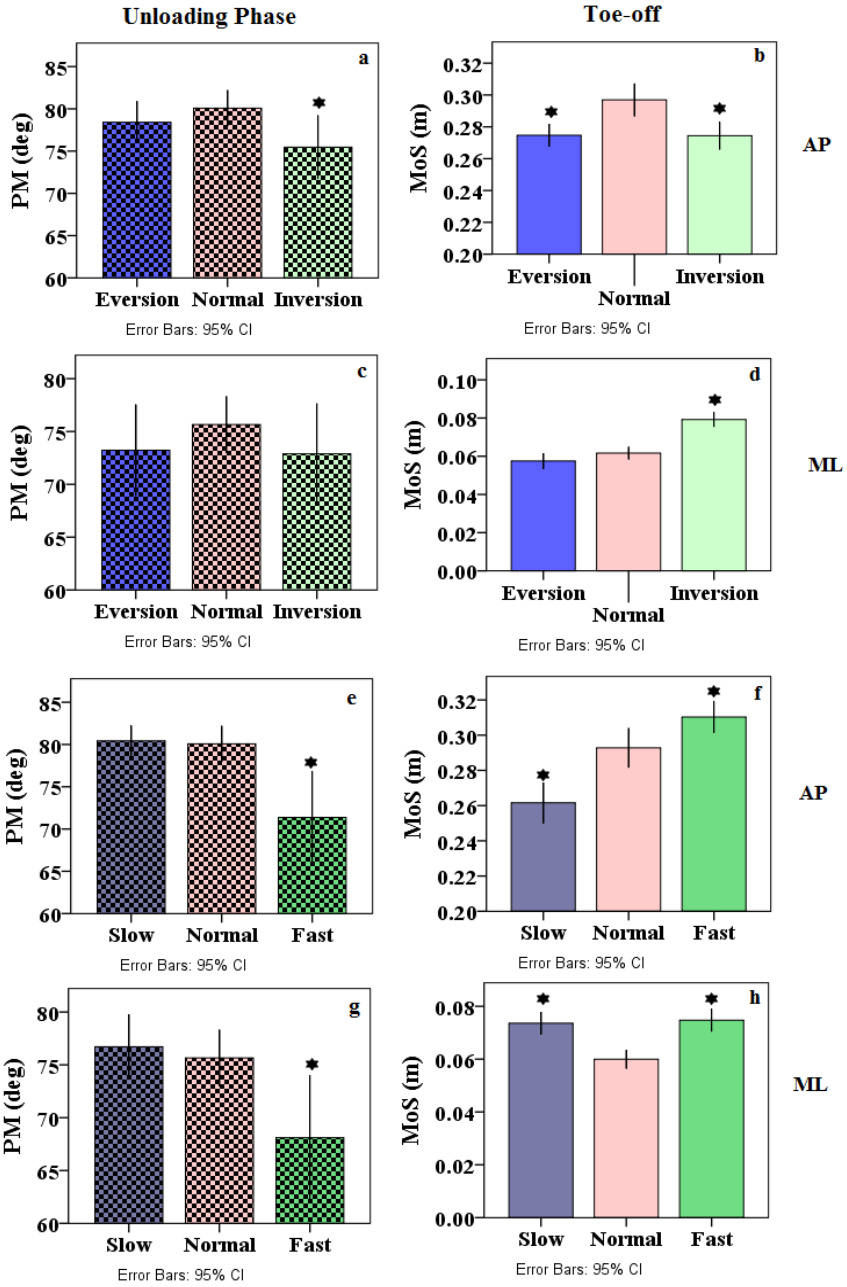

Fig. 4. Instability margins comparison during unloading phases applying N&B methods (left) and extrapolated-CoM method (right). (a-d) rotational impairments in anterior-posterior (AP) and medial-lateral (ML) directions, (e-h) walking speed group in AP and ML directions, * shows significant ($p<0.05$) difference.

Comparatively, the best-fit CoM-oscillations (I/P) models illustrated unstable responses during both loading and unloading phases (Table A2) in AP direction. In a rotational group, the instability (PM) was increased in an everted foot walk during loading and in an inverted foot walk during the unloading phase. During loading phases, a walk at fast speed showed an increase ($p<0.05$) in instability in terms of PMs, and during unloading, a slow speed walk

decreased ($p<0.05$) in instability. However, the instability quantified by GMs at fast speed decreased ($p<0.05$) during loading and increased in unloading phases. Stability margins quantified from I/Ps were compared with one from O/Ps for each of the walking conditions as illustrated in Fig. 5.

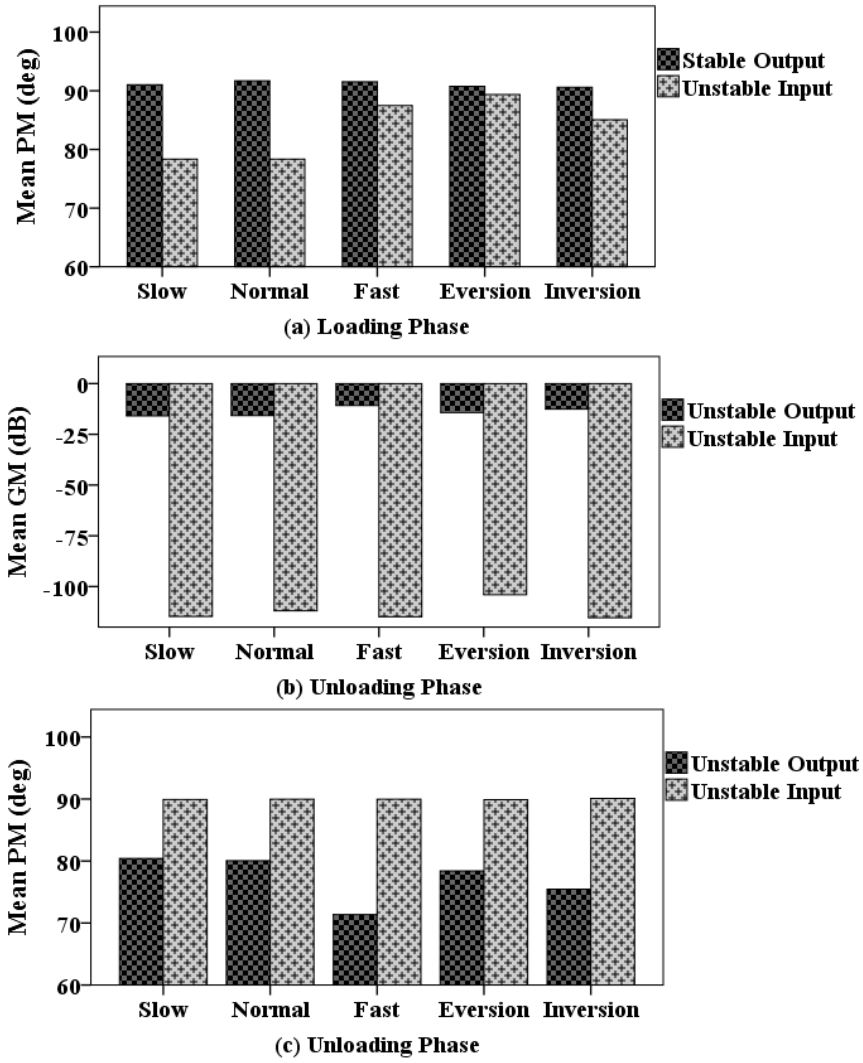

Fig 5. Comparison of neuromotor outputs and inputs. Stability margins quantified from the neuromotor output (CoP-velocity) and input (CoM-oscillation) responses in the anterior-posterior direction. The input instability is greater than outputs in all walking conditions.

An intralimb interaction between loading and unloading phases CoP-velocities (Table 1) showed strong negative correlations between them with $p<0.001$ in respective walking conditions. However, there was no correlation found between CoP-velocity and CoM-oscillations during both loading and unloading phases.

Table 1. Spearman's correlation between opposite limbs loading and unloading phases.

Walking Conditions	**Normal** (p-value)	**Eversion*** (p-value)	**Inversion*** (p-value)	**Slow** (p-value)	**Fast** (p-value)
Anterior-posterior	-0.809 (0.001)	-0.834 (0.001)	-0.779 (0.001)	-0.864 (0.001)	-0.778 (0.001)

Medial-lateral	-0.842 (0.001)	-0.812 (0.001)	-0.791 (0.001)	-0.777 (0.001)	-0.772 (0.001)

*Symmetric restrictions applied for both right and left foot.

4. Discussion

This study evaluates dynamic stability during gait transitional phases applying Nyquist and Bode (N&B) methods. Overall results illustrated significant differences in stability margins with the effect of self-selected walking speeds and rotational impairments. In this study, walking stabilities are evaluated using resultant neuromechanical O/I signals i.e. CoP and CoM-acceleration that provide redundancy in measurements compared with multiple signals being used earlier. Further, N&B methods used a distinct cut-off (0dB, $\pm 180° \pm 2k\pi$) to define and quantify stable or unstable gait phases independent to comparing with control subjects. This implies that the stability definitions are standardized rather being dependent on fluctuating references. The phase margins quantified applying N&B methods are also compared with extrapolated-CoM method, however, the former evaluates stabilities within gait phases (loading and unloading) and the later evaluates discrete gait events (HC, TO) which present start and endpoints of respective phases.

Studies regarding neuromotor control reported the independence of CoP signals from CoM (Winter, 2009). Our results confirmed this statistically and illustrated poor correlation (Spearman's correlations) between these two signals. This biological fact helps to analyse both signals independently. The methodological steps defined here for CoP or CoM-acceleration based stability analysis are adopted from literature with waveforms having similar time-varying characteristics (Anderson et al., 2009; Downes et al., 2012). The most important one is the linear model identification for the plant. A plant model is identified from lower limb balance control signals i.e. CoP measures resultant neuromotor output and CoM-acceleration measures somatosensory feedback which counts almost 70% (Bekkers et al., 2014) of all neuromotor feedbacks. The time rate-of-change illustrated impulsive nature characteristics of measured O/I signals, that enable us to quantify the time and amplitude differences between normal and other simulated walking conditions. The PCA applied here to clean the O/I signals illustrated a low dimensionality that helps to approximate plant O/Is as linear regression models following (Anderson et al., 2009). Prior studies analyse CoP/CoM signals in the time domain and stability outcomes are reported for the whole gait cycle in terms of either range-of-motion (ROM) (Lugade & Kaufman, 2014) or the time constant and residual instability (Cattaneo et al., 2014; Rabuffetti et al., 2011). The methods define here quantify gait transitional phases i.e. weight loading and unloading gait sub-phases which are critical in muscles activation and hence in neuromotor balance control. In this study, a frequency domain analysis to the modelled signals provides a way to extract important balance control differentials (i.e time differences as PM and amplitude differences as GM) with standard set criteria.

The stability margins from neuromechanical O/P illustrated loading phases as stable and unloading phases as unstable. This is consistent with extrapolated-CoM method in which XCoM was reported within BoS at heel contact as a measure of stability and swayed outside the BoS at toe-off gave a measure of instability (Lugade et al., 2011). Further, our results illustrated a strongly negative correlation between opposite limb loading and unloading phases CoP-velocities (O/P). Both loading and unloading phases took place in parallel but out of

phase. This correlation illustrates that one limb during its loading phase (stable) is used to compensate for the opposite limb's unloading phase (unstable) by an intralimb interaction. This interaction is also reported earlier in elderly subjects which used their leading limb to compensate the reduced push-off from trailing limb (Hernández, Silder, Heiderscheit, & Thelen, 2009). However, there was no correlation found between rate dependant CoP and CoM-acceleration waveforms which showed their independence consistent with findings reported by Winter (Winter, 2009).

The results from rotational impairments showed a decrease in stability margins in loading phases observed both in anterior-posterior and medial-lateral directions. That was due to the reduced area during foot contact (HC) with the floor in these conditions (Õunpuu et al., 2013). These findings were also determined to be consistent with event-based MoS(s) evaluations. Overall, the inverted foot was found least stable in this group with decreased PM(s) both in AP and ML directions. Previously, the inverted ankle sprain is described as the most sensitive sports injury and has a chronic contribution towards gait instability (Hernández et al., 2009).

During respective unloading phases, our methods showed a decrease in inverted foot instability in the forward direction (AP). That is consistent with outcomes reported in lateral ankle sprains patients who were observed reluctantly to put bodyweight at the forefoot (Ihlen et al., 2012). However, the MoS(s) applying extrapolated-CoM method showed a decrease in MoS(s) at TO event (poor balance control) compared to a normal walk. In the medial-lateral direction, N&B stability methods showed decreasing trends in instability for both inversion and eversion, however, remained statistically insignificant whereas MoS illustrated an increase in instability in the inverted foot. These contradictions between GMs and MoS(s) might be due to the consideration of CoM along with CoP in MoS evaluations that increases/decreases the sensitivity of measurements whereas N&B methods analysed CoP and CoM signals independently as a neuromotor O/I. Our methods (N&B) illustrated that the rotational impairments significantly affected gait transitional stabilities with a decrease in stabilities during loading and decrease in instability during unloading phases.

The effect of walking speed on gait dynamic stability is reported earlier with inconsistent outcomes e.g. slow walking speed is reported more stable in one study and negated in another (Bruijn, van Dieën, Meijer, & Beek, 2009; Gigi et al., 2015). The stability margins quantified here at self-selected walking speed showed that a normal/preferred speed walk was more stable (PM) than a slow walk and had no difference with fast speed during the loading phase. This finding is consistent with studies (Fan, Li, Han, Lv, & Zhang, 2016; Kavanagh, 2009) in which a preferred walking speed showed the best compromise for frontal plane stability during single limb support and smooth weight transfer during double limb support. A self-selected normal walking speed is also reported to conserve the transformation energies (kinetic to potential and vice versa) during gait transitions (Beyaert, Vasa, & Frykberg, 2015; Lu, Kuo, Chang, Lu, & Hong, 2017). During respective unloading phases, a decrease in instability at fast speed walk made its preference over slow and normal speed walks which did not illustrate any mutual difference. This is consistent with findings from a prior study in which a fast speed walk is reported with increased stability considering entire gait cycle waveforms applying local dynamic stability method (Lu, Lu, Lin, Hsieh, & Chan, 2017). The extrapolated-CoM also supported these findings with increased MoS(s) at fast speed in both AP and ML directions. Applying N&B stability measures, the conclusions may be drawn that the normal and fast

walking speeds are equally stable during loading phases and a fast speed walk decrease in instability during the unloading phase of double limb support.

A comparison between stability outcomes from neuromotor O/Is i.e. CoP-velocity and CoM-oscillations illustrated that during loading phases, the outputs have more stable and less unstable margins (magnitudes) compared with respective inputs during both loading and unloading phases as illustrated earlier in Fig. 5. Furthermore, the gain margins quantified applying N&B methods illustrated the robustness of O/I impulsive responses in terms of magnitudes. During loading, all walking conditions showed infinite GMs which means neuromotor control is robust enough to accommodate large perturbations while loading. This was also illustrated during the respective unloading phases in which there is a significant decrease in input GMs observed compared with outputs. That increase in output's stability during loading and decrease in output's instability during the unloading illustrates the neuromotor balance control ability in response to somatosensory inputs.

4.1. Limitations

Unlike in MoS evaluations, the N&B methods are appropriate for dynamic gait assessments and are not suitable for a static gait. These methods are sensitive to best-fit models applying system identification as a small compromise in best fit can result in a large difference in stability margins. This study evaluated anterior-posterior GRFs as a somatosensory input, however, the vertical GRF having maximum magnitudes are needed to be investigated in future. Lastly, the walking speeds are evaluated for over ground trials which increase the variance among the participants at each preferred speed. Treadmill based trials are speculated to illustrate further stability differences during gait transitional phases.

5. Conclusions

Stability margins evaluated during gait transitional phases illustrated significant differences in loading phases and partially affected unloading phases. The rotational impairments significantly decreased stabilities during loading phases both in AP and ML directions and only inverted foot illustrated decrease in forward instability during the unloading phase. A slow speed walk showed a decrease in loading stability and a fast speed walk illustrated a decrease in instability during the unloading phase of double limb support. The methods described in the current manuscript also illustrate the neuromotor balance control ability quantified distinctly from input and output responses. The N&B methods provide an alternative stability assessment technique with the advantage of distinct criteria and evaluation of gait subphase. The use of resultant neuromechanical signals makes these methods potentially suitable for stability evaluation in either type of lower limb impairments, with/without wearable devices, and walking on varying terrains.

6. Declarations of interest:

None.

Acknowledgements

The corresponding author would like to thank his PhD scholarship sponsor, University of Engineering and Technology, Lahore, Pakistan. The authors would like to thank all the participants and lab staff.

548 **Appendix A: Supplementary Figures and Tables**

549

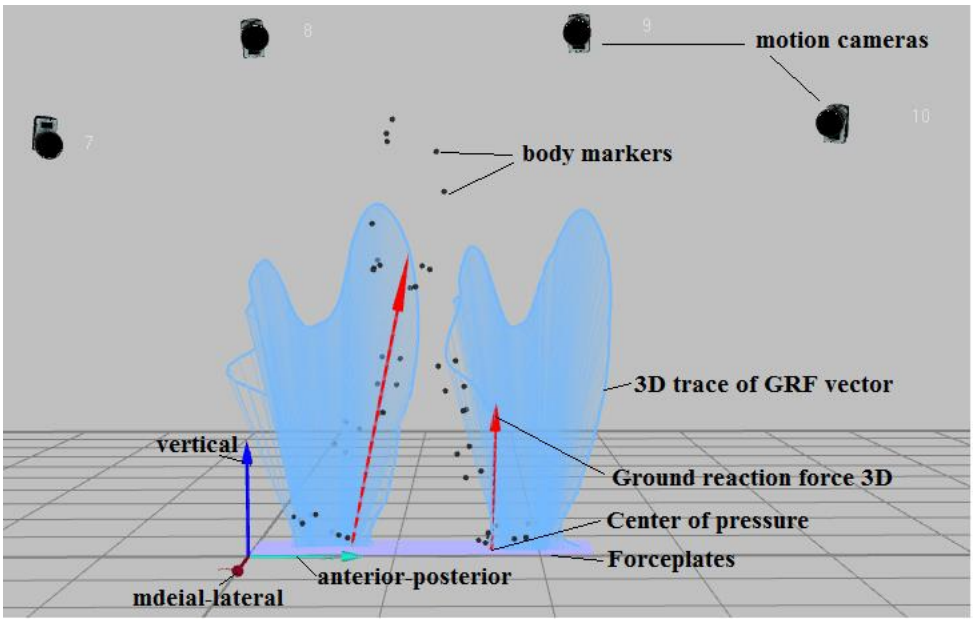

550

551 **Figure A.1 Motion capture system and measurement signals illustrating ground**
552 **reaction force vector trace with tail presenting centre of pressure trajectory and vector**
553 **head present CoM-acceleration (GRF/mass).**

554

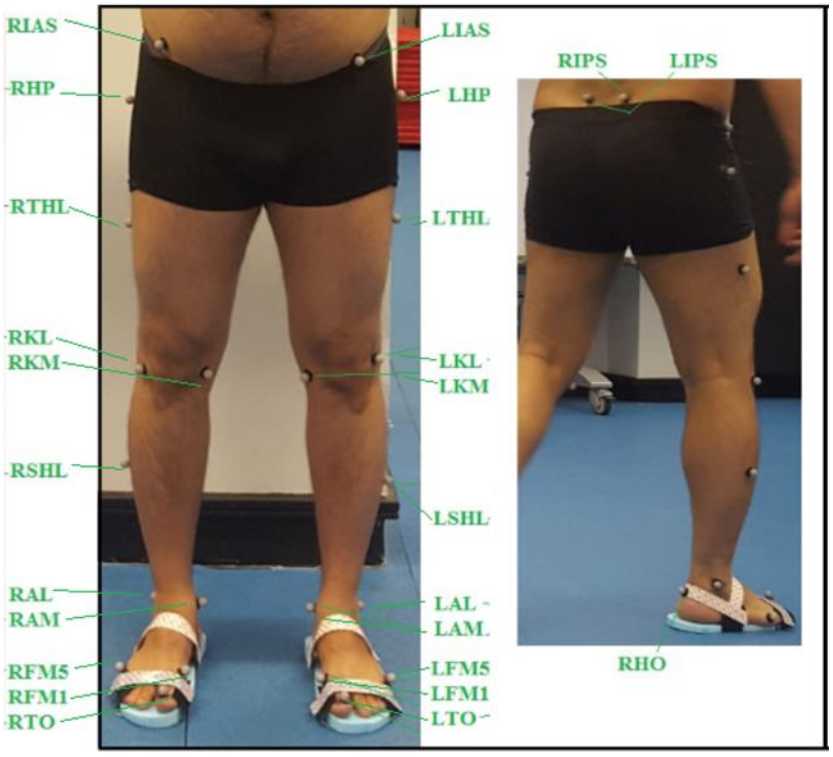

555

556 **Figure A.2 Markers placement at lower-limbs anatomical positions illustrated.**

557

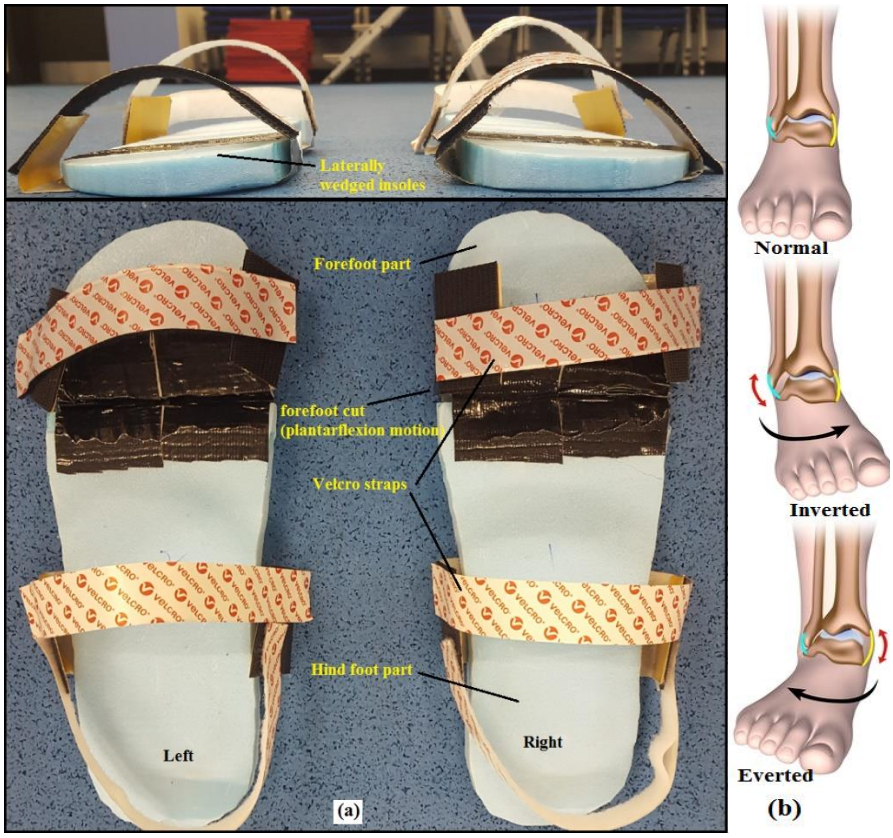

Figure A.3 (a) Wedged insoles illustrated for inverted foot walk, (b) rotational foot abnormalities illustrated, fig. adopted from https://www.oastaug.com/ankle-sprains-high-vs-low/.

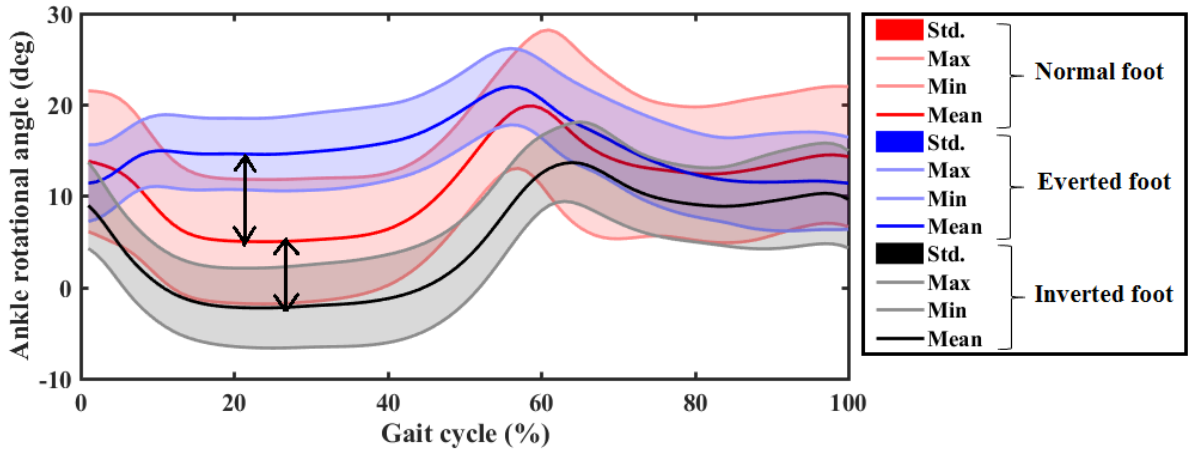

Figure A.4 Ankle-foot rotational angles illustrated for the normal and simulated inverted and everted foot conditions. A maximum difference(arrows) between the normal-everted foot and normal-inverted foot trajectories illustrate the rotational angles obtained experimentally in response to wedged foot insoles.

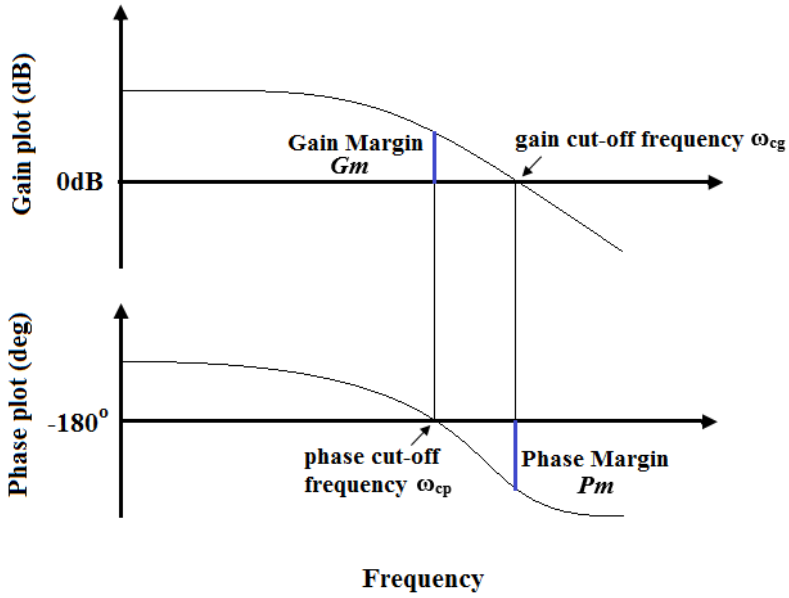

(a) Bode plots

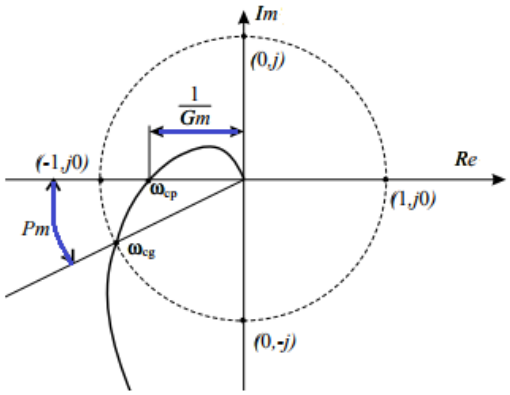

(b) Nyquist plot

Figure A.5 Bode plots and equivalent Nyquist plot illustrating distinct references, cut-off frequencies and stability margins.

Table A.1 Stability margins quantified from CoP-velocity and MoS(s) for walking speed and rotational impairments.

Walking Conditions	GM (dB)	PM (deg)	MoS-HC (m)	GM (dB)	PM (deg)	MoS-TO (m)
Anterior-posterior						
Normal	∞	91.7 1.27	0.296 0.032	-15.78 3.14	80.07 3.18	0.292 0.026
Slow	∞	**91.03** 0.45	0.289 0.04	-15.91 2.51	80.42 3.18	**0.261** 0.03
Fast	∞	91.53 0.86	0.301 0.025	**-10.79** 4.01	**71.38** 8.12	**0.304** 0.024
Eversion	∞	**90.75** 0.32	**0.273** 0.021	-14.33 2.58	78.41 3.71	**0.268** 0.031
Inversion	∞	**90.59** 0.21	**0.273** 0.027	**-12.58** 3.21	**75.46** 5.61	**0.270** 0.023
Medial-lateral						
Normal	∞	92.28 1.45	0.0494 0.008	-12.45 2.52	75.65 3.98	0.0609 0.013
Slow	∞	**91.51** 0.81	**0.0604** 0.0132	-13.26 3.06	76.71 4.58	**0.0734** 0.008
Fast	∞	91.92 1.12	**0.0612** 0.008	**-9.27** 3.41	**68.11** 8.8	**0.0747** 0.013
Eversion	∞	**91.14** 0.40	**0.0316** 0.011	-11.40 3.26	73.22 6.44	0.0566 0.014
Inversion	∞	**91.0** 0.38	**0.0606** 0.013	-11.27 3.26	72.89 7.07	**0.079** 0.013

Bold values showing $p<0.05$ when compared with a normal walk. Mean walking speeds i.e. Normal (1.132 m/s), Slow (0.86 m/s), and Fast (1.356 m /s).

Table A.2 Stability margins quantified from CoM-oscillations for walking speed and rotational impairments.

Walking Condition	GM (dB)	PM (deg)	GM (dB)	PM (deg)
Normal	-148.66 6.75	78.36 12.90	-111.96 2.33	89.963 0.009
Slow	-148.66 6.75	78.36 12.90	-114.72 3.75	**89.917** 0.023
Fast	**-141.30** 3.46	**87.48** 2.42	**-114.87** 2.66	89.973 0.012
Eversion	**-133.11** 3.91	**89.37** 2.27	-104.03 9.46	**89.899** 0.11
Inversion	-142.53 7.56	85.06 3.59	**-115.37** 2.16	**90.101** 0.308

Bold values showing $p<0.05$ when compared with a normal walk.

Appendix B: Abbreviations

BoS	base of support
CoM	centre of mass
CoP	centre of pressure
deg	degree (unit of angle)
dB	decibel (unit of gain)
GM	gain margin
GRF	ground reaction force
I/P	input
LTI	linear time-invariant
MoS	margin of stability
N&B	Nyquist and Bode
O/I	output/input
O/P	output
PCA	principal component analysis
PM	phase margin
R^2	coefficient of determinant
ROM	range of motion
Std.	standard deviation
TF	transfer function
XCoM	extrapolated CoM

References

Allen, J. L., & Ting, L. H. (2016). Why Is Neuromechanical Modeling of Balance and Locomotion So Hard? In B. I. Prilutsky & D. H. Edwards (Eds.), *Neuromechanical Modeling of Posture and Locomotion* (pp. 197-223). New York, NY: Springer New York.

Anderson, S. R., Porrill, J., Sklavos, S., Gandhi, N. J., Sparks, D. L., & Dean, P. (2009). Dynamics of Primate Oculomotor Plant Revealed by Effects of Abducens Microstimulation. *Journal of Neurophysiology, 101*(6), 2907-2923. doi: 10.1152/jn.91045.2008

Ardestani, M. M., ZhenXian, C., Noori, H., Moazen, M., & Jin, Z. (2019). Computational Analysis of Knee Joint Stability Following Total Knee Arthroplasty. *Journal of Biomechanics*. doi: https://doi.org/10.1016/j.jbiomech.2019.01.029

Bavafa-Toosi, Y. (2017). 6 - Nyquist plot. In Y. Bavafa-Toosi (Ed.), *Introduction to Linear Control Systems* (pp. 471-575): Academic Press.

Bekkers, E. M. J., Dockx, K., Heremans, E., Vercruysse, S., Verschueren, S. M. P., Mirelman, A., & Nieuwboer, A. (2014). The contribution of proprioceptive information to postural control in elderly and patients with Parkinson's disease with a history of falls. *Frontiers in human neuroscience, 8*, 939-939. doi: 10.3389/fnhum.2014.00939

Beyaert, C., Vasa, R., & Frykberg, G. E. (2015). Gait post-stroke: Pathophysiology and rehabilitation strategies. *Neurophysiologie Clinique/Clinical Neurophysiology, 45*(4), 335-355. doi: http://dx.doi.org/10.1016/j.neucli.2015.09.005

Bizovska, L., Svoboda, Z., Kutilek, P., Janura, M., Gaba, A., & Kovacikova, Z. (2014). Variability of centre of pressure movement during gait in young and middle-aged women. *Gait & Posture, 40*(3), 399-402. doi: https://doi.org/10.1016/j.gaitpost.2014.05.065

Blum, K. P., Lamotte D'Incamps, B., Zytnicki, D., & Ting, L. H. (2017). Force encoding in muscle spindles during stretch of passive muscle. *PLOS Computational Biology, 13*(9), e1005767. doi: 10.1371/journal.pcbi.1005767

Bruijn, S. M., van Dieën, J. H., Meijer, O. G., & Beek, P. J. (2009). Is slow walking more stable? *Journal of Biomechanics, 42*(10), 1506-1512. doi: https://doi.org/10.1016/j.jbiomech.2009.03.047

C-Motion_Angles. (2019). https://c-motion.com/v3dwiki/index.php/Tutorial:_Foot_and_Ankle_Angles

C-Motion_Markers. (2019). https://www.c-motion.com/v3dwiki/index.php/Marker_Set_Guidelines#Model_1.

Cattaneo, D., Rabuffetti, M., Bovi, G., Mevio, E., Jonsdottir, J., & Ferrarin, M. (2014). Assessment of postural stabilization in three task oriented movements in people with multiple sclerosis. *Disability and Rehabilitation, 36*(26), 2237-2243. doi: 10.3109/09638288.2014.904933

Cohen, M. X. (2014). *Analyzing neural time series data: theory and practice - Chapter 23*: MIT press.

DiDomenico, A., McGorry, R. W., & Banks, J. J. (2013). Methodological considerations of existing techniques for determining stabilization times following a multi-planar transition. *Gait & Posture, 38*(3), 541-543. doi: http://dx.doi.org/10.1016/j.gaitpost.2013.01.011

Downes, T. P., Welch, D., Scott, K. S., Austermann, J., Wilson, G. W., & Yun, M. S. (2012). Calculating the transfer function of noise removal by principal component analysis and application to AzTEC deep-field observations. *Monthly Notices of the Royal Astronomical Society, 423*(1), 529-542. doi: 10.1111/j.1365-2966.2012.20896.x

Fan, Y., Li, Z., Han, S., Lv, C., & Zhang, B. (2016). The influence of gait speed on the stability of walking among the elderly. *Gait & Posture, 47*, 31-36. doi: https://doi.org/10.1016/j.gaitpost.2016.02.018

Gigi, R., Haim, A., Luger, E., Segal, G., Melamed, E., Beer, Y., . . . Elbaz, A. (2015). Deviations in gait metrics in patients with chronic ankle instability: a case control study. *Journal of Foot and Ankle Research, 8*(1), 1. doi: 10.1186/s13047-014-0058-1

Graham, D. F., Carty, C. P., Lloyd, D. G., & Barrett, R. S. (2017). Muscle contributions to the acceleration of the whole body centre of mass during recovery from forward loss of balance

by stepping in young and older adults. *PLOS ONE, 12*(10), e0185564. doi: 10.1371/journal.pone.0185564

Hernández, A., Silder, A., Heiderscheit, B. C., & Thelen, D. G. (2009). Effect of age on center of mass motion during human walking. *Gait & Posture, 30*(2), 217-222. doi: https://doi.org/10.1016/j.gaitpost.2009.05.006

Hof, A. L. (2008). The 'extrapolated center of mass' concept suggests a simple control of balance in walking. *Human Movement Science, 27*(1), 112-125. doi: https://doi.org/10.1016/j.humov.2007.08.003

Hur, P., Duiser, B. A., Salapaka, S. M., & Hsiao-Wecksler, E. T. (2010). Measuring Robustness of the Postural Control System to a Mild Impulsive Perturbation. *IEEE Transactions on Neural Systems and Rehabilitation Engineering, 18*(4), 461-467. doi: 10.1109/TNSRE.2010.2052133

Ihlen, E. A. F., Goihl, T., Wik, P. B., Sletvold, O., Helbostad, J., & Vereijken, B. (2012). Phase-dependent changes in local dynamic stability of human gait. *Journal of Biomechanics, 45*(13), 2208-2214. doi: https://doi.org/10.1016/j.jbiomech.2012.06.022

ImageJ-macros. (2019). http://dev.mri.cnrs.fr/projects/imagej-macros/wiki/Velocity_Measurement_Tool

Inspect3D. (2018). https://www.c-motion.com/v3dwiki/index.php/Inspect3D_Overview. 2018.

Kang, H. G., & Dingwell, J. B. (2009). Dynamics and stability of muscle activations during walking in healthy young and older adults. *Journal of Biomechanics, 42*(14), 2231-2237. doi: https://doi.org/10.1016/j.jbiomech.2009.06.038

Kavanagh, J. J. (2009). Lower trunk motion and speed-dependence during walking. [journal article]. *Journal of NeuroEngineering and Rehabilitation, 6*(1), 9. doi: 10.1186/1743-0003-6-9

La Scaleia, V., Ivanenko, Y. P., Zelik, K. E., & Lacquaniti, F. (2014). Spinal motor outputs during step-to-step transitions of diverse human gaits. *Frontiers in Human Neuroscience, 8*, 305. doi: 10.3389/fnhum.2014.00305

Lencioni, T., Rabuffetti, M., Piscosquito, G., Pareyson, D., Aiello, A., Di Sipio, E., . . . Ferrarin, M. (2014). Postural stabilization and balance assessment in Charcot–Marie–Tooth 1A subjects. *Gait & Posture, 40*(4), 481-486. doi: https://doi.org/10.1016/j.gaitpost.2014.07.006

Lu, H.-L., Kuo, M.-Y., Chang, C.-F., Lu, T.-W., & Hong, S.-W. (2017). Effects of gait speed on the body's center of mass motion relative to the center of pressure during over-ground walking. *Human Movement Science, 54*, 354-362. doi: https://doi.org/10.1016/j.humov.2017.06.004

Lu, H.-L., Lu, T.-W., Lin, H.-C., Hsieh, H.-J., & Chan, W. P. (2017). Effects of belt speed on the body's center of mass motion relative to the center of pressure during treadmill walking. *Gait & Posture, 51*, 109-115. doi: https://doi.org/10.1016/j.gaitpost.2016.09.030

Lugade, V., & Kaufman, K. (2014). Center of pressure trajectory during gait: A comparison of four foot positions. *Gait & Posture, 40*(4), 719-722. doi: http://dx.doi.org/10.1016/j.gaitpost.2014.07.001

Lugade, V., Lin, V., & Chou, L.-S. (2011). Center of mass and base of support interaction during gait. *Gait & posture, 33*(3), 406-411.

Maslivec, A., Bampouras, T. M., Dewhurst, S., Vannozzi, G., Macaluso, A., & Laudani, L. (2018). Mechanisms of head stability during gait initiation in young and older women: A neuro-mechanical analysis. *Journal of Electromyography and Kinesiology, 38*, 103-110. doi: https://doi.org/10.1016/j.jelekin.2017.11.010

Mei, Z., Zhao, G., Ivanov, K., Guo, Y., Zhu, Q., Zhou, Y., & Wang, L. (2013). Sample entropy characteristics of movement for four foot types based on plantar centre of pressure during stance phase. [journal article]. *BioMedical Engineering OnLine, 12*(1), 101. doi: 10.1186/1475-925x-12-101

Morgan, K. D., Zheng, Y., Bush, H., & Noehren, B. (2016). Nyquist and Bode stability criteria to assess changes in dynamic knee stability in healthy and anterior cruciate ligament reconstructed individuals during walking. *Journal of Biomechanics, 49*(9), 1686-1691. doi: http://dx.doi.org/10.1016/j.jbiomech.2016.03.049

Neptune, R., & Vistamehr, A. (2018). Dynamic Balance during Human Movement: Measurement and Control Mechanisms. *Journal of Biomechanical Engineering*. doi: 10.1115/1.4042170

Õunpuu, S., Garibay, E., Solomito, M., Bell, K., Pierz, K., Thomson, J., . . . DeLuca, P. (2013). A comprehensive evaluation of the variation in ankle function during gait in children and youth with Charcot–Marie–Tooth disease. *Gait & Posture, 38*(4), 900-906. doi: https://doi.org/10.1016/j.gaitpost.2013.04.016

Portela, F. M., Rodrigues, E. C., & de Sá Ferreira, A. (2014). A critical review of position-and velocity-based concepts of postural control during upright stance. *Human Movement, 15*(4), 227-233.

Rabiei, M., Eslami, M., & Movaghar, A. F. (2016). The assessment of three-dimensional foot pronation using a principal component analysis method in the stance phase of running. *The Foot, 29*, 11-17. doi: https://doi.org/10.1016/j.foot.2016.09.008

Rabuffetti, M., Bovi, G., Quadri, P. L., Cattaneo, D., Benvenuti, F., & Ferrarin, M. (2011). An experimental paradigm to assess postural stabilization: no more movement and not yet posture. *IEEE Transactions on Neural Systems and Rehabilitation Engineering, 19*(4), 420-426.

Robbins, S. M., Astephen Wilson, J. L., Rutherford, D. J., & Hubley-Kozey, C. L. (2013). Reliability of principal components and discrete parameters of knee angle and moment gait waveforms in individuals with moderate knee osteoarthritis. *Gait & Posture, 38*(3), 421-427. doi: https://doi.org/10.1016/j.gaitpost.2013.01.001

Sivakumaran, S., Schinkel-Ivy, A., Masani, K., & Mansfield, A. (2018). Relationship between margin of stability and deviations in spatiotemporal gait features in healthy young adults. *Human Movement Science, 57*, 366-373. doi: https://doi.org/10.1016/j.humov.2017.09.014

Sklavos, S., Porrill, J., Kaneko, C. R. S., & Dean, P. (2005). Evidence for wide range of time scales in oculomotor plant dynamics: Implications for models of eye-movement control. *Vision Research, 45*(12), 1525-1542. doi: https://doi.org/10.1016/j.visres.2005.01.005

Soares, D. P., de Castro, M. P., Mendes, E., & Machado, L. (2014). Influence of wedges on lower limbs' kinematics and net joint moments during healthy elderly gait using principal component analysis. *Human Movement Science, 38*, 319-330. doi: https://doi.org/10.1016/j.humov.2014.09.007

Svoboda, Z., Bizovska, L., Janura, M., Kubonova, E., Janurova, K., & Vuillerme, N. (2017). Variability of spatial temporal gait parameters and center of pressure displacements during gait in elderly fallers and nonfallers: A 6-month prospective study. *PLOS ONE, 12*(2), e0171997. doi: 10.1371/journal.pone.0171997

Tan, M. H., & Hammond, J. K. (2007). A non-parametric approach for linear system identification using principal component analysis. *Mechanical Systems and Signal Processing, 21*(4), 1576-1600. doi: https://doi.org/10.1016/j.ymssp.2006.07.005

van der Linden, M. H., van der Linden, S. C., Hendricks, H. T., van Engelen, B. G. M., & Geurts, A. C. H. (2010). Postural instability in Charcot-Marie-Tooth type 1A patients is strongly associated with reduced somatosensation. *Gait & Posture, 31*(4), 483-488. doi: https://doi.org/10.1016/j.gaitpost.2010.02.005

Winter, D. A. (2009). *Biomechanics and motor control of human movement*: John Wiley & Sons.